J|A|C|S COMMUNICATIONS

Published on Web 05/12/2009

Low-Energy Networks of the T-Cage $(H_2O)_{24}$ Cluster and Their Use in Constructing Periodic Unit Cells of the Structure I (sI) Hydrate Lattice

Soohaeng Yoo,[†] Mikhail V. Kirov,[‡] and Sotiris S. Xantheas*,[†]

Chemical & Materials Sciences Division, Pacific Northwest National Laboratory, P.O. Box 999, MS K1-83, Richland, Washington 99352, and Institute of the Earth Cryosphere, Siberian Branch of the Russian Academy of Sciences, 625000 Tyumen, Russia

Received February 12, 2009; E-mail: sotiris.xantheas@pnl.gov

Hydrate crystal structures are water scaffolds held together by hydrogen bonds that can act as "host" lattices by trapping "guest" molecules such as Cl_2, Br_2, SO_2, H_2S, and CH_4 within their cages via weak van der Waals interactions.[1−3] The potential importance of clathrate hydrates (i.e., the combination of the host lattice and the guest molecules) as inclusion compounds relevant to renewable energy (i.e., molecular hydrogen storage devices) has recently been emphasized.[4−8] A bottleneck in the modeling of these networks lies with the existence of a plethora $[(^3/_2)^N]$ of possible isomers satisfying the Bernal−Fowler ice rules[9] based on the position of the H atoms. Here we report the structure and vibrational spectra of the global minimum and low-energy networks of the tetrakaidecahedral cage (T-cage) $(H_2O)_{24}$ cluster via a hierarchical approach that offers a path toward identifying the low-energy networks for larger cages. We furthermore outline a "bottom-up" procedure for constructing three-dimensional (3D) periodic networks of the structure I [denoted (sI)] hydrate lattice starting from any of the low-energy networks of the T-cage.

All of the natural gases that form clathrate hydrates do so in the following three crystal structures:[10,11] (sI) (cubic, $Pm\bar{3}n$), (sII) (cubic, $Fd\bar{3}m$), and (sH) (hexagonal, $P6/mmm$). These 3D lattices are formed by a combination of the following building blocks (cages): (*i*) the pentagonal dodecahedron (D-cage), consisting of 20 water molecules forming 12 pentagonal faces (5^{12}); (*ii*) the T-cage, consisting of 24 water molecules forming 12 pentagonal and 2 hexagonal faces ($5^{12}6^2$); (*iii*) the hexakaidecahedron (H-cage), consisting of 28 water molecules forming 12 pentagonal and 4 hexagonal faces ($5^{12}6^4$); (*iv*) the irregular dodecahedron, consisting of 20 water molecules forming 3 tetragonal, 6 pentagonal, and 3 hexagonal faces ($4^35^66^3$); and (*v*) the icosahedron, consisting of 36 water molecules that form 12 pentagonal and 8 hexagonal faces ($5^{12}6^8$). The unit cell of the (sI) hydrate comprises two units of 5^{12} and six units of $5^{12}6^2$ cages. The unit cell of the (sII) hydrate comprises 16 units of 5^{12} and eight units of $5^{12}6^4$ cages. The (sII) hydrate has been shown to meet current U.S. Department of Energy's target densities for an on-board hydrogen storage system.[7,12] Finally, the unit cell of the (sH) hydrate consists of three units of 5^{12}, two units of $4^35^66^3$, and one unit of $5^{12}6^8$ cages.

Even though the constituent cages of the (sI), (sII), and (sH) hydrates are well-known from X-ray crystallography, the energy-preferred topology of the H-bond network is still unknown, unlike those of other naturally occurring non-H-containing clathrate structures such as melanophlogite.[13] This is the case because even for their smaller constituent gas-phase cages, the number of symmetry-distinct configurations emanating from the different hydrogen positions consistent with the ice rules is quite large: 30 026 for the 5^{12} D-cage $(H_2O)_{20}$,[14] 3 043 836 for the $5^{12}6^2$ T-cage $(H_2O)_{24}$, and 61 753 344 for the $5^{12}6^4$ H-cage $(H_2O)_{28}$ gas-phase clusters.[15] Because of this obstacle, previous calculations[16−18] have relied on a "top-down" approach in which the hydrate lattice was constructed from the known positions of the O atoms and randomly selected H positions satisfying the ice rules, maximizing the H-bonding network, and yielding a zero total dipole moment according to the procedure delineated for hexagonal ice.[19] This procedure is, however, based on a statistical sampling of proton disordered networks, requires very large (>1000 molecule) supercells even for nominally small unit cells (4 molecules/unit cell for ice Ih), and is not practical for hydrate structures where the unit cells are much larger [46 and 136 molecules for structures (sI) and (sII), respectively]. It also does not guarantee that either the most stable or the low-lying hydrate networks will be constructed. In contrast, our approach can be considered as "bottom-up", as it starts from the low-energy networks of the constituent cages and moves up to the 3D lattice of the hydrate.

We employed a four-step hierarchical procedure to determine the global minimum and the low-energy networks of the T-cage $(H_2O)_{24}$ cluster: (*i*) All of the possible 3 043 836 symmetry-distinct configurations were classified into groups using the strong−weak effective bond (SWEB) discrete model,[20,21] depending on the maximum number of the strongest hydrogen bonds. The SWEB model explicitly defines an "effective" nearest-neighbor (*n*-*n*) interaction based on the relative (*n*-*n*) orientation and the connectivity to second- and third-neighbor molecules.[21] It is assumed that the most stable networks have the maximum number of strong effective H-bonds, an assumption previously justified[21] for the D-cage, where the total number of networks (30 026) is more tractable. For the T-cage $(H_2O)_{24}$ cluster, there are 321 symmetry-distinct isomers with a maximum number of 9 "strong" H-bonds. (*ii*) The relative energies of those 321 low-lying candidates predicted with the SWEB model were refined via geometry optimizations with the TIP4P,[22] TTM2.1-F,[23] and TTM3-F[24] interaction potentials for water. (*iii*) The 66 lowest-energy networks obtained from the classical water potential results were refined by full geometry optimization at the density functional theory (DFT) level. The DFT calculations employed Becke's gradient-corrected exchange-correlation density functional (B3LYP)[25,26] and Ahlrichs' polarized valence triple-ζ (TZVP) basis set.[27] (*iv*) The final list of low-energy networks was determined by full geometry optimization of the first 18 low-lying DFT minina at the second-order Møller−Plesset (MP2) perturbation theory[28] level with Dunning's augmented correlation-consistent basis sets of double- and triple-ξ quality (aug-cc-pVDZ and aug-cc-pVTZ, respectively).[29,30] The number of networks considered at each step was determined by the grouping of isomers (usually a break in their relative energies) obtained at

[†] Pacific Northwest National Laboratory.
[‡] Institute of the Earth Cryosphere.

10.1021/ja9011222 CCC: $40.75

the previous step. All of the electronic structure calculations were performed with the NWChem suite of codes.[31]

Schlegel diagrams[32] (2D projections of the 3D structures) of the 10 lowest-energy minima of the T-cage (fully optimized at the MP2/aug-cc-pVDZ level of theory) are shown in Figure 1. The various

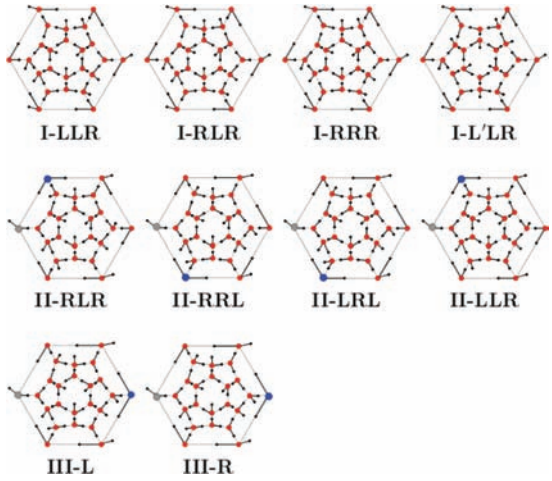

Figure 1. Schlegel diagrams of the 10 lowest minima of the T-cage $(H_2O)_{24}$ cluster obtained at the MP2/aug-cc-pVDZ level of theory.

networks are labeled using **R** or **L** for each of the three concentric rings starting from the inner one, depending on whether the direction of the donor H atoms in the ring is clockwise (**R**) or counterclockwise (**L**). For example, the **RLR** isomer has a clockwise arrangement of the H atoms in the inner and outer circles and a counterclockwise direction in the middle circle. The **L′LR** isomer has the same ring directions as **LLR** but differs in the direction of the vertical H atoms. These 10 lowest-energy minima can be furthermore grouped into three families (denoted as **I**, **II**, and **III**), depending on the connectivity of the top hexagonal face (hydrogen bonded six-membered ring). Family **I** isomers have only acceptor−donor (AD) water molecules on the hexagonal face, while family **II** and **III** isomers have double-donor (DD) and double-acceptor (AA) water molecules on the hexagonal face (blue and gray dots, respectively, in Figure 1). For the family **III** isomers, only the direction of the inner ring is denoted, as there is no uniform **R/L** pattern in the middle and outer rings. All 10 minima have a zero total dipole moment. Their relative order (shown in Figure 1) with respect to the most stable network, **I-LLR**, network is exactly the same with the larger aug-cc-pVTZ basis set (see Figure 1 and Table 1 in the Supporting Information).

We computed the harmonic vibrational frequencies of the 10 low-energy minima of the T-cage at the B3LPY/TZVP level of theory. The harmonic IR spectra in the OH stretch region (2400−4000 cm^{-1}) for the three families **I**−**III**, shown in Figure 2a−c, were fitted with a Lorentzian line shape using a half-width at half-maximum of 10 cm^{-1}. All 10 minima exhibit a most red-shifted, IR-active band centered at ∼2750 cm^{-1}. This band arises from the OH stretching vibrations within the middle ring of the Schlegel diagrams, as shown in Figure 2d for the family **I** isomers. A notable difference for families **II** and **III** is the existence of an additional band (indicated by the shaded area) at ∼2930 cm^{-1} that is absent for the family **I** isomers. This additional band is due to the vibrations of the DD and AA water molecules that lie on the hexagonal face and arises from the vertical OH stretching vibrations between the middle layer and the top AA (or DD) water molecule, as shown in Figure 2e,f for families **II** and **III**, respectively. The positions of those most red-shifted IR-active bands are consistent

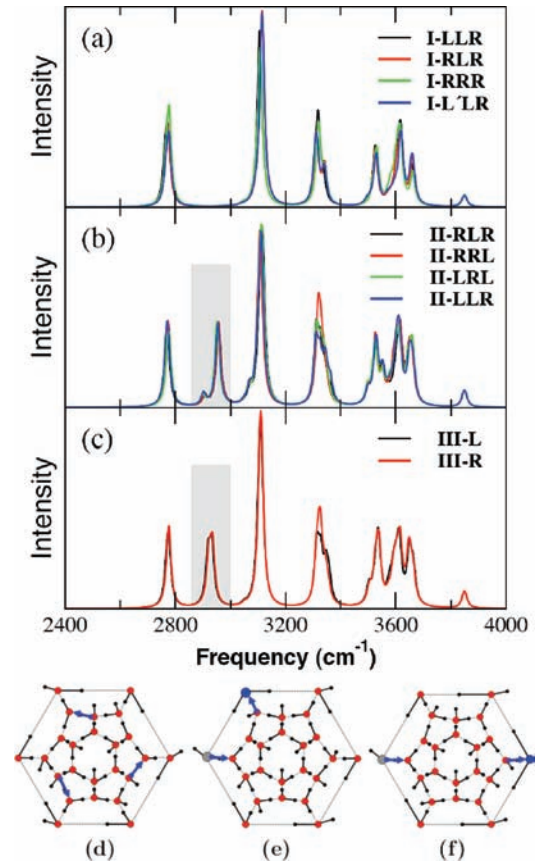

Figure 2. (top) Harmonic IR spectra of (a) family **I**, (b) family **II**, and (c) family **III** isomers in the OH-stretching region obtained at the B3LYP/TZVP level of theory. (bottom) Normal mode displacement vectors for the most red-shifted band at ∼2750 cm^{-1} for (d) family **I** isomers and the band at ∼2930 cm^{-1} for (e) family **II** and (f) family **III** isomers.

with the experimentally measured spectra for crystalline hydrates of HCl, HBr,[33] and H_2SO_4,[34] which exhibit overlapping bands in the 2900−3100 cm^{-1} range.

On the basis of the information on the low-energy networks of the T-cage, our proposed "bottom-up" approach can now be employed in order to design unit cells of the (sI) hydrate crystal structure. This approach is further justified by previous reports suggesting that the most stable nanostructures are built from the low-lying networks of their constituent building blocks.[35−37] For example, elongated structures of silicon clusters were built from their magic-number clusters Si_6 and Si_{10}, while spherical ones were built from fullerene cages.[36,37] In the same manner, the 46-molecule (sI) hydrate cubic unit cell results in a periodic lattice in which a nucleus of two adjacent T-cages is surrounded by six D-cages. If two low-lying T-cages sharing a common hexagonal face are used as the building blocks for this nucleus, then the positions of the hydrogen atoms of 36 molecules ($2 \times 24 - 6 - 6$) are determined. In this manner, the number of possible networks of the (sI) hydrate unit cell is dramatically reduced. The proposed approach used to design low-lying hydrogen bonding networks of the unit cell of the (sI) hydrate is schematically illustrated in Figure 3. Any of the low-lying networks of the T-cage can be used as the starting point. Here we illustrate this process starting from the lowest-lying isomer, **I-LLR**: the first step (Figure 3a) is to insert this isomer into a cubic unit cell (blue-shaded box) and its neighboring unit cell (indicated by **LLR** in the blue-colored neighbor unit). The two cages are stitched together by a network of O atoms, initially without any H atoms, indicated by gray color in Figure 3a. The second step is to

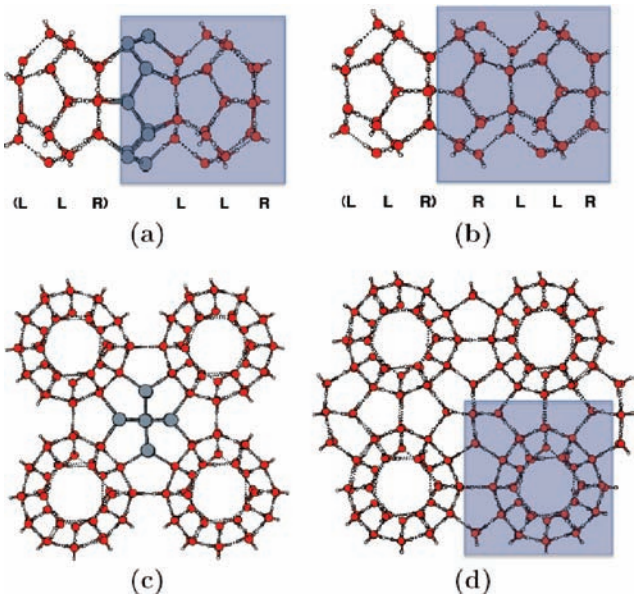

Figure 3. Schematic approach for building the (sI) hydrate lattice from low-lying networks of the T-cage. Connecting O atoms between the two cages (without hydrogen atoms) are highlighted in gray. The blue box indicates the (sI) cubic unit cell (46 atoms).

identify the hydrogen arrangement of these gray-colored connecting O atoms. Even though there are numerous possible hydrogen arrangements, we used the **I-RRL** isomer, as it is the mirror image of the initial **I-LLR** isomer (and therefore has the same energy) and also satisfies the hydrogen arrangements on the top and bottom hexagonal rings. After addition of **I-RRL** between two **I-LLR** T-cages, the −**RLLR**− pattern is formed in the *z* direction, as indicated by the blue colored box in Figure 3b (choosing **L** for the connecting O atoms yields a higher-energy network instead). Within these first two steps, the positions of the hydrogen atoms for 36 water molecules (among the 46 in the cubic unit cell) are already determined. In Figure 3c, the −**RLLR**− building block of two connected T-cages is replicated in the *x* and *y* directions in order to determine the hydrogen arrangement of the remaining 10 water molecules in the unit cell. In fact, there is only one possible arrangement of the H atoms for the remaining 10 water molecules. Figure 3d depicts a supercell of (sI) hydrate with zero total dipole moment. In a similar manner, several (sI) hydrate supercells can be built starting from the other low-energy networks of the T-cage. The relative stability of those periodic networks will be the subject of a future study.

In summary, we have relied on a hierarchical screening procedure in order to identify the lowest-lying isomers of the T-cage ($5^{12}6^2$) water cluster, which is a constituent cage in the (sI) hydrate lattice. Furthermore, we have outlined a procedure for constructing 3D periodic networks of the (sI) hydrate lattice starting from any of these low-energy networks of the T-cage. When the lowest-lying isomer, **I-LLR**, is used as the building block of the (sI) hydrate lattice, the possible configurations in the cubic unit cell are dramatically reduced, resulting in a network with better physical stability. This work will enable the design of hydrate lattices for the modeling of guest−host interactions in clathrate hydrate structures.

Acknowledgment. Part of this work was supported by the Russian Foundation for Basic Research (Grant 08-03-0-00338) and by the Division of Chemical Sciences, Biosciences and Geosciences, U.S. Department of Energy. Battelle operates the Pacific Northwest National Laboratory for the U.S. Department of Energy. This research was performed in part using the Molecular Science Computing Facility (MSCF) in the Environmental Molecular Sciences Laboratory, a national scientific user facility sponsored by the Department of Energy's Office of Biological and Environmental Research.

Supporting Information Available: A table and figure showing the MP2/aug-cc-pVDZ and MP2/aug-cc-pVTZ//MP2/aug-cc-pVDZ total and relative energies and the B3LYP/TZVP zero-point energy corrections. This material is available free of charge via the Internet at http://pubs.acs.org.

References

(1) Sloan, E. D. *Clathrate Hydrates of Natural Gases*, 2nd ed.; Marcel Dekker: New York, 1998.
(2) Sloan, E. D. *Nature* **2003**, *426*, 353.
(3) Strobel, T. A.; Hester, K. C.; Sloan, E. D., Jr.; Koh, C. A. *J. Am. Chem. Soc.* **2007**, *129*, 9544.
(4) Schlapbach, L.; Züttel, A. *Nature* **2001**, *414*, 353.
(5) Mao, W. L.; Mao, H. K.; Goncharov, A. F.; Struzhkin, V. V.; Guo, Q.; Hu, J.; Shu, J.; Hemley, R. J.; Somayazulu, M.; Zhao, Y. *Science* **2002**, *297*, 2247.
(6) Florusse, L. J.; Peters, C. J.; Schoonman, J.; Hester, K. C.; Koh, C. A.; Dec, S. F.; Marsh, K. N.; Sloan, E. D. *Science* **2004**, *306*, 469.
(7) Schüth, F. *Nature* **2005**, *434*, 712.
(8) Lee, H.; Lee, J. W.; Kim, D. Y.; Park, J.; Seo, Y. T.; Zeng, H.; Moudrakovski, I. L.; Ratcliffe, C. I.; Ripmeester, J. A. *Nature* **2005**, *434*, 743.
(9) Bernal, J. D.; Fowler, R. H. *J. Chem. Phys.* **1933**, *1*, 515.
(10) Jeffrey, G. A.; McMullan, R. K. *Prog. Inorg. Chem.* **1967**, *8*, 43.
(11) Ripmeester, J. A.; Tse, J. S.; Ratcliffe, C. I.; Powell, B. M. *Nature* **1987**, *325*, 135.
(12) Mao, W. L.; Mao, H. K.; Meng, Y.; Eng, P. J.; Hu, M. Y.; Chow, P.; Cai, Y. Q.; Shu, J.; Hemley, R. J. *Science* **2006**, *314*, 636.
(13) Kortus, J.; Irmer, G.; Monecke, J.; Pederson, M. R. *Model. Simul. Mater. Sci. Eng.* **2000**, *8*, 403.
(14) McDonald, S.; Ojamäe, L.; Singer, S. J. *J. Phys. Chem.* **1998**, *102*, 2824.
(15) Kirov, M. V. *J. Struct. Chem.* **2002**, *43*, 790.
(16) van Klaveren, E. P.; Michels, J. P. J.; Schouten, J. A.; Klug, D. D.; Tse, J. S. *J. Chem. Phys.* **2001**, *114*, 5745.
(17) Dornan, P.; Alavi, S.; Woo, T. K. *J. Chem. Phys.* **2007**, *127*, 124510.
(18) Peters, B.; Zimmermann, N. E.; Beckham, G. T.; Tester, J. W.; Trout, B. L. *J. Am. Chem. Soc.* **2008**, *130*, 17342.
(19) Buch, V.; Sandler, P.; Sadlej, J. *J. Phys. Chem. B* **1998**, *102*, 8641.
(20) Kirov, M. V. *J. Struct. Chem.* **2005**, *46*, S188.
(21) Kirov, M. V.; Fanourgakis, G. S.; Xantheas, S. S. *Chem. Phys. Lett.* **2008**, *461*, 180.
(22) Jorgensen, W. L.; Chandrasekhar, J.; Madura, J. D.; Impey, R. W.; Klein, M. L. *J. Chem. Phys.* **1983**, *79*, 926.
(23) Fanourgakis, G. S.; Xantheas, S. S. *J. Phys. Chem. A* **2006**, *110*, 4100.
(24) Fanourgakis, G. S.; Xantheas, S. S. *J. Chem. Phys.* **2008**, *128*, 074506.
(25) Becke, A. D. *Phys. Rev. A* **1988**, *38*, 3098.
(26) Becke, A. D. *J. Chem. Phys.* **1993**, *98*, 5648.
(27) Schäfer, A.; Huber, C.; Ahlrichs, R. *J. Chem. Phys.* **1994**, *100*, 5829.
(28) Møller, C.; Plesset, M. S. *Phys. Rev.* **1934**, *46*, 618.
(29) Dunning, T. H. *J. Chem. Phys.* **1989**, *90*, 1007.
(30) Kendall, R. A.; Dunning, T. H.; Harrison, R. J. *J. Chem. Phys.* **1992**, *96*, 6796.
(31) Kendall, R. A.; Aprà, E.; Bernholdt, D. E.; Bylaska, E. J.; Dupuis, M.; Fann, G. I.; Harrison, R. J.; Ju, J.; Nichols, J. A.; Nieplocha, J.; Straatsma, T. P.; Windus, T. L.; Wong, A. T. *Comput. Phys. Commun.* **2000**, *128*, 260.
(32) Schlegel, V. *Verh. Kais. Leopold.-Carolin. Dtsch. Akad. Naturforsch.* **1883**, *44*, 343.
(33) Delzeit, L.; Rowland, B.; Devlin, J. P. *J. Phys. Chem.* **1993**, *97*, 10312.
(34) Nash, K. L.; Sully, K. J.; Horn, A. B. *J. Phys. Chem. A* **2001**, *105*, 9422.
(35) Ho, K. M.; Shvartsburg, A. A.; Pan, B.; Lu, Z. Y.; Wang, C. Z.; Wacker, J. G.; Fye, J. L.; Jarrold, M. F. *Nature* **1998**, *392*, 582.
(36) Yoo, S.; Zhao, J.; Wang, J.; Zeng, X. C. *J. Am. Chem. Soc.* **2004**, *126*, 13845.
(37) Yoo, S.; Zeng, X. C. *Angew. Chem., Int. Ed.* **2005**, *44*, 1491.

JA9011222